Four-Point Bending Tests of Ductile Iron Pipe with Insituform IMain Liner

Prepared by

Cornell University NEESR Group

September 7, 2011

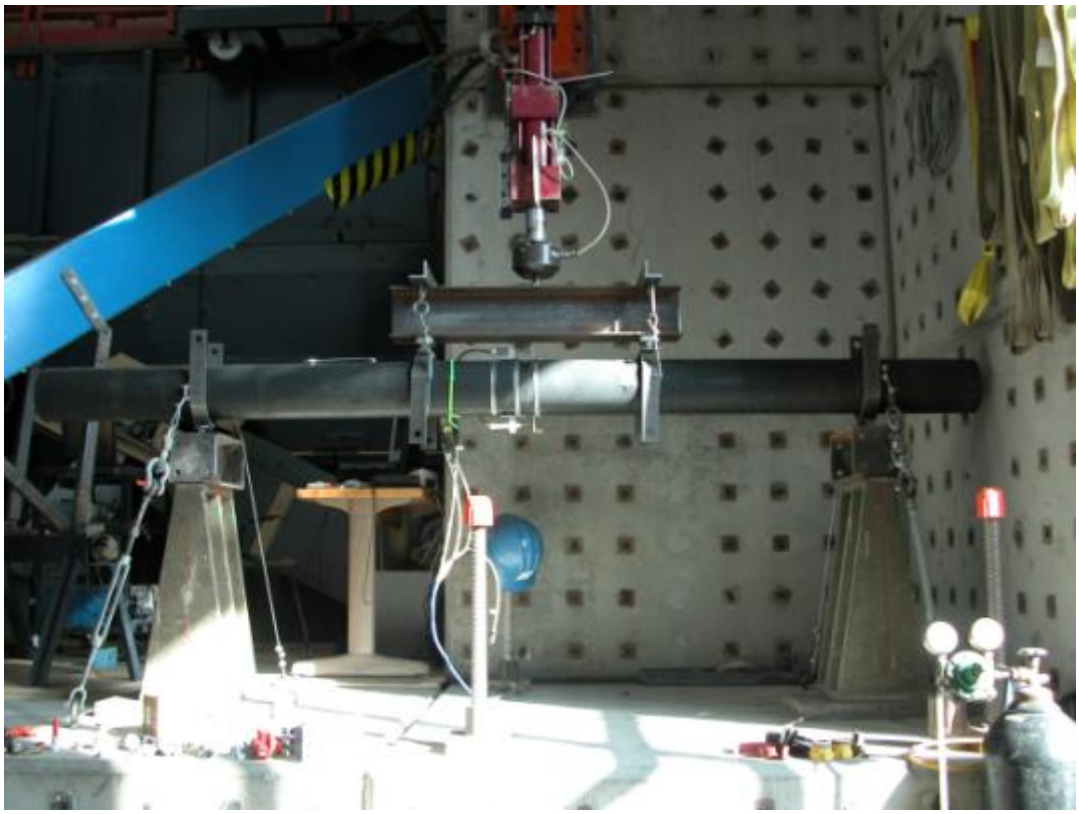

TABLE OF CONTENTS

Table of Contents i
List of Tables i
List of Photos ii
List of Figures ii

1. Introduction 3
2. Theory 4
3. Setup and Procedure 7
4. Data and Results 9
    4.1 Specimen 1 10
    4.2 Specimen 2 14
    4 .3 Specimen 3 17
    4.4 Specimen 10 22
    4.5 Specimen 12 26
5. Discussion of Results 30
6. Summary and Recommendations 33

LIST OF TABLES

Table 1. Bending Test Specimens 9
Table 2. Target Test Regimen for Specimen 1 10
Table 3. Target Test Regimen for Specimen 2 14
Table 4. Target Test Regimen for Specimen 3 18
Table 5. Target Test Regimen for Specimen 10 22
Table 6. Target Test Regimen for Specimen 12. 27
Table 7. Summary of Approximate Specimen Stiffness 30

LIST OF PHOTOS

Photo 1. Test Apparatus for Four-Point Bending Test 5
Photo 2. Image of Specimen 1 Liner after First Rotation Testing 12
Photo 3. Image of the Specimen 2 Liner after First Rotation Testing 15
Photo 4. Image of Specimen 3 Liner after First Rotation 20
Photo 5. Image of Specimen 10 Liner after First Rotation Testing 24
Photo 6. Image of the Specimen 12 Liner after First Rotation Testing 28

LIST OF FIGURES

Figure 1. Ductile Iron Joint Cross-section 4
Figure 2. Schematic of Four-Point Bending Test 5
Figure 3. Force vs. Displacement for Specimen 1 11
Figure 4. Peak Force vs. Displacement for Specimen 1 13
Figure 5. Moment vs. Rotation for Specimen 1 13
Figure 6. Force vs. Displacement for Specimen 2 15
Figure 7. Peak Force vs. Displacement for Specimen 2 16
Figure 8. Moment vs. Rotation for Specimen 2 17
Figure 9. Force vs. Displacement for Cycles 1-5, Specimen 3 18
Figure 10. Force vs. Displacement for Cycles 6 – 10, Specimen 3 19
Figure 11. Peak Force vs. Displacement for Specimen 3 21
Figure 12. Moment vs. Rotation for Specimen 3 21
Figure 13 : Force vs. Displacement for Cycles 1 – 7, Specimen 10. 23
Figure 14 : Force vs. Displacement for Cycles 8 - 11, Specimen 10. 24
Figure 15 : Peak Force vs. Displacement for Specimen 10. 25
Figure 16 : Moment vs. Rotation for Specimen 10. 26
Figure 17 : Force vs. Displacement for Specimen 12. 27
Figure 18 : Peak Force vs. Displacement for Specimen 12. 29
Figure 19 : Moment vs. Rotation for Specimen 12. 29
Figure 20 : Force-displacement based on peak points for Specimens 1 and 2. 31
Figure 21 : Force-displacement based on peak points for Specimens 1, 2 and 10. 32
Figure 22. Force-displacement based on peak points for Specimens 3 and 12. 33

1. Introduction

Four-point bending tests were performed on several sections of 152 mm (6 in.) nominal diameter ductile iron (DI) pipe sections lined with InsituForm IMain pipe liners. The composition of the liner was IMain epoxy resin with IMain hardener. The goal of the tests was to characterize the flexural strength and failure mechanics of lined DI pipes considering varying composite interfaces and discontinuities.

The standard DI pipes used in the tests were provided by LADWP (Los Angeles Department of Water & Power) and sent to InsituForm Technologies (Chesterfield, MO) to be lined with IMain liner technology and cut to a prescribed length. Twelve specimens were shipped to Cornell University for use in the four-point bending tests (Specimens 1, 2, 3, 10, and 12) and axial pull tests (Specimens 4 – 9 and 11). The Axial Pull tests are discussed in a separate document ("Axial Pull Test of InsituForm IMain Liner" prepared by Cornell University NEESR Group, September 2011.)

Four-point bending specimens were prepared at nominal lengths of 2.4 m (8 ft). Before the IMain liner was applied the pipes consisted of ductile iron with a wall thickness approximately 7.6 mm (0.30 in.) thick and an interior mortar lining approximately 3.3 mm (0.13 in.) thick. The outer and inner diameters of the unlined pipes were respectively 175 mm (6.87 in.) and 153 mm (6.01 in.) (see Figure 1). With an average thickness of 6.50 mm (0.256 in.) the IMain liner reduced the inner diameter of the lined pipes to approximately 144.5 mm (5.69 in.).

Four different sample types were prepared and tested including joint and gap centered sections. Jointed sections consist of a standard bell and spigot connection sealed with a greased rubber gasket (see Figure 1). The center of the joint, or approximate location of bell and spigot end contact, was centered below the actuator. The second sample type consisted of a length of pipe with a full circumferential break at mid length. The specimen was cut into two pieces prior to lining and then aligned for the lining process. This type of specimen was intended to simulate a previously broken or cracked pipe that was repaired by introduction of the liner. These are referred to as "gap" specimens.

When the IMain liner is applied in the field, the curing process results in a bond between the outside of the liner and the mortar at the inside face of the pipe. In an effort to better understand the effect of this bond half of the samples were prepared as they would be in the field with a bond between liner and pipe. The other half were prepared with a polyethylene bond breaker sheet

installed between the liner and the inside wall of the pipe as an attempt to prevent the formation of this bond.

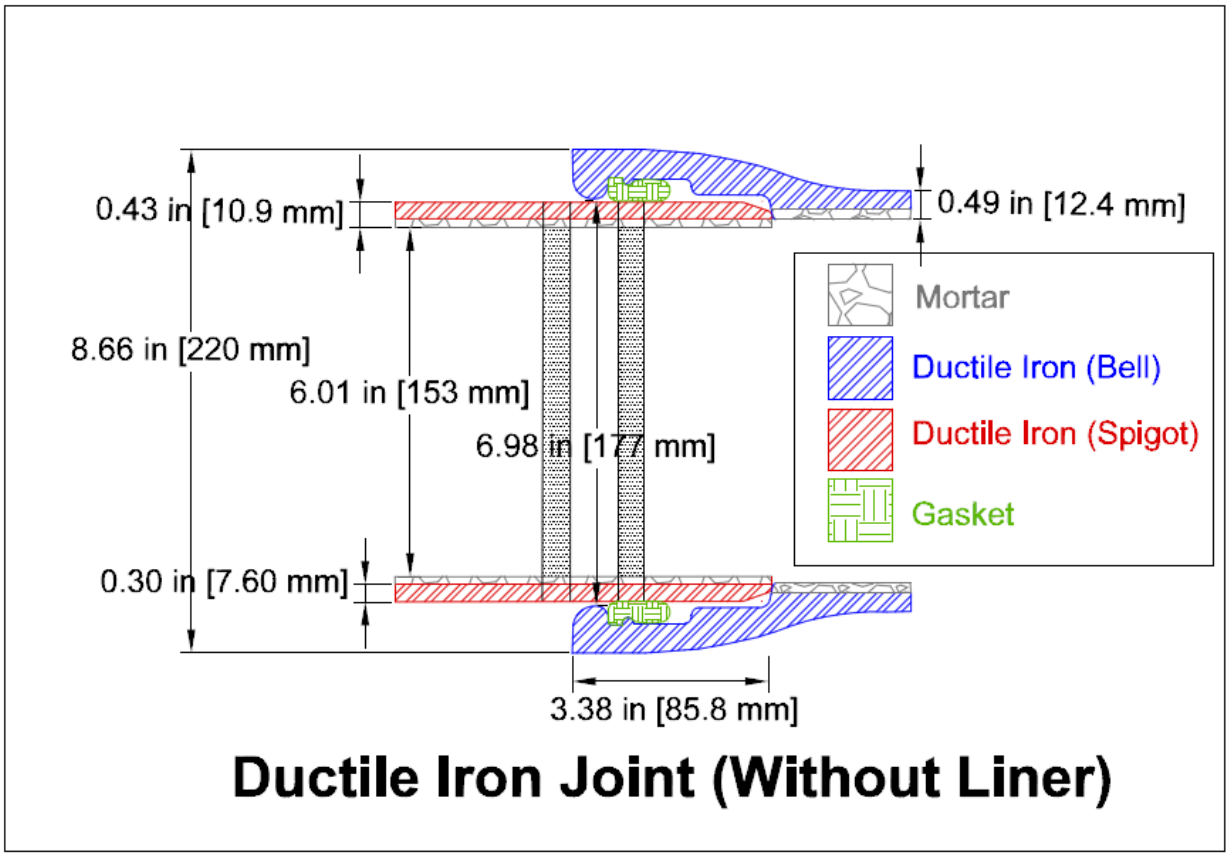

Figure 1. Ductile Iron Joint Cross-section

2. Theory

Four-point bending tests, as shown in Photo 1, were performed to allow testing at the center of the sample under constant applied moment and zero shear. Figure 2 demonstrates the four-point bending test load, shear, and moment diagrams. The uniform moment across the center of the pipe sections is:

$$M = \frac{FL}{6} \tag{1}$$

in which:

F = Actuator force, and

L = total length of pipe section between outermost supports.

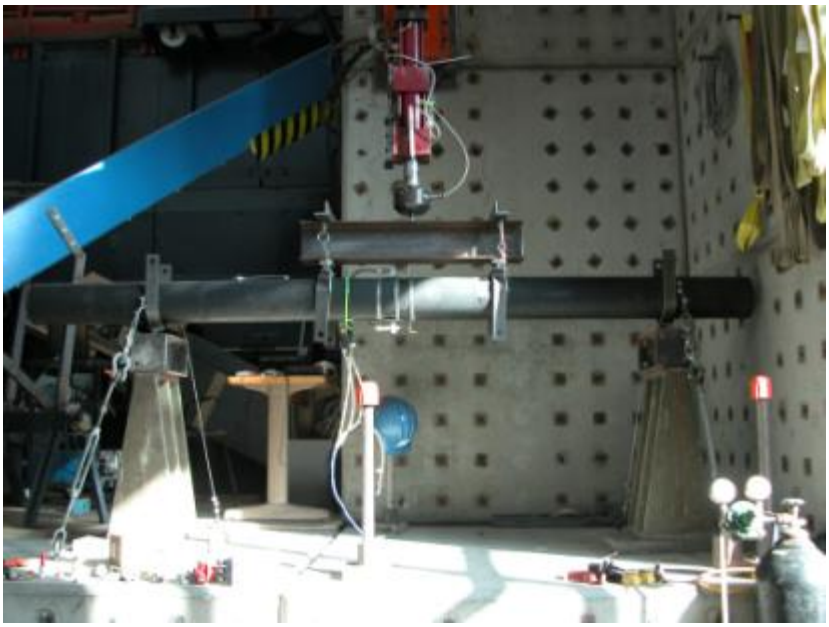

Photo 1. Test Apparatus for Four-Point Bending Test

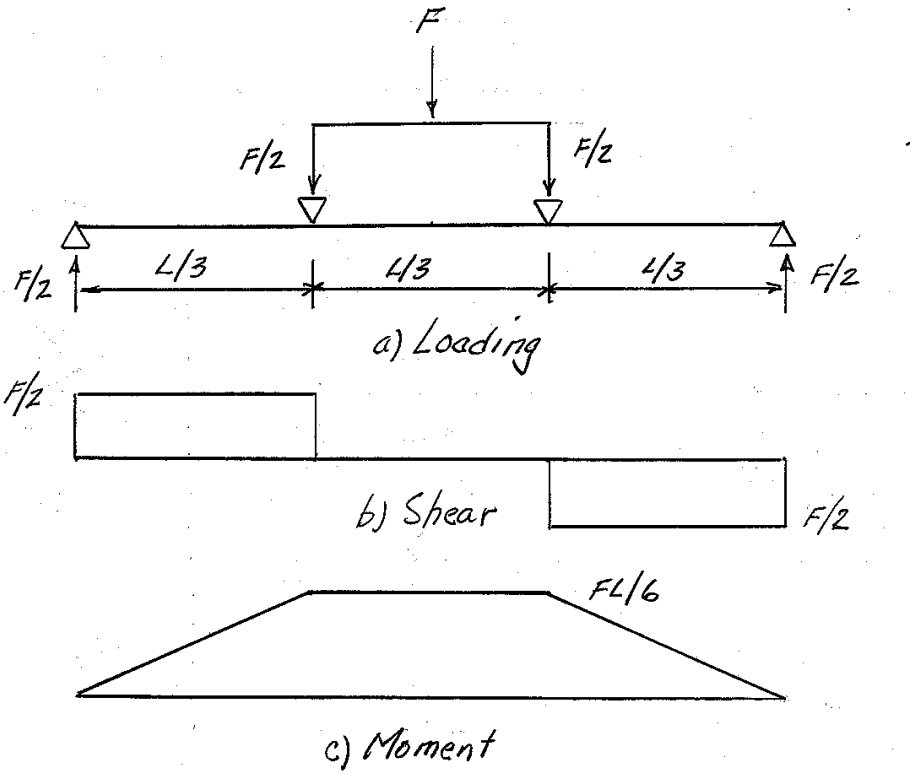

Figure 2. Schematic of Four-Point Bending Test

The lined four-point bending pipe sections were loaded at locations such that equal dimensions of L/3 were equal to 710 mm (28 in.). The distances from the actuator to upper load points were identically spaced at 355 mm (14 in.).

According to ASCI (American Institute of Steel Construction, 2007), the maximum deflection due to bending is related to the applied force as shown in Equation 2 below. This equation was manipulated to provide an estimate of the initial bending stiffness, EI, of the test specimens.

$$\delta = \frac{Fa}{24EI}\left(3L^2 - 4a^2\right) \quad (2)$$

where:

F = ½ of Applied Actuator force

L = Total length of pipe section between outermost supports

E = Young's modulus of the composite cross section

I = Cross-section moment of inertia

a = Distance along pipe between loading point and closest outer support = L/3

The average inner diameter of the five lined four-point bending pipes was $(D_i)_{avg}$ = 144.5 mm (5.689 in.). Previous Ring Tests on the lining material revealed an average wall thickness of t_w = 6.50 mm (0.256 in.). The minimum wall thickness measured in the ring specimens was 5.12 mm (0.205 in.). The maximum wall thickness was 9.91 mm (0.390 in.) at one of the stitched sections. The maximum thickness for each ring specimen was always at a stitched section. The ring test specimens were cast in Sonotubes of the same lining material used in the lined DI pipes. The average outside diameter of the ring specimens was 152.4 mm (6.00 in.), the diameter of the Sonotube. More detailed description of the ring specimens is presented in the "Ring Compression Tests of Insituform IMain Liner" report prepared by Cornell University NEESR Group in September, 2011.

The outer diameter of the composite liner was assumed to have the same average thickness and inner diameter as the Ring Test specimens previously described. Measurements of the four point bending specimens confirmed this assumption. Using these properties the outer diameter of the section is give as:

$$D_o = (D_i)_{avg} + 2\,t_w = 5.689 + 2 *(0.256) = 6.201 \text{ in.} \quad (3)$$

The moment of inertia, I, of the liner is given by:

$$I = \frac{\pi\,(D_O^4 - D_i^4)}{64} = \frac{\pi\,(6.201^4 - 5.689^4)}{64} = 21.162\ in.^4 \quad (4)$$

The distance to the outer fiber of the liner is:

$$c = D_O / 2 = D_i / 2 + t_W = 3.357 \text{ in.} \quad (5)$$

The maximum outer fiber stress is:

$$\sigma_{max} = \frac{M\,c}{I} = \frac{F_{max}\,L}{6}\frac{c}{I} \quad (6)$$

Rearrange to:

$$F_{max} = \frac{6\,\sigma_{max}\,I}{L\,c} \quad (7)$$

Based on data obtained from InsituForm the mean IMain flexural strength in the axial direction is $(\sigma_b)_{max}$ = 13830 psi.

Setting $\sigma_{max} = (\sigma_b)_{max}$ = 13830 psi and solve for $F_{max} \approx$ 6230 lb.

3. Setup and Procedure

The general procedure for the testing is given below.

1) Place the specimen on the support stands, with the original North/South markers at top dead center,
2) Align the specimen with the load apparatus,
3) Connect the cable and come-along tie downs at the end supports,
4) Connect, align and center the measuring instruments which include one DCDT at the crown of the pipe measuring from the spigot to the bell, one at the invert and a clinometer at the spring line of the pipe,
5) Set and align the saddles for the load spreader,
6) Extend the actuator and spreader to just touch the blocks above the saddles,
7) Apply a downward deflection of 0.050 in. (using 0.001 in. steps),

8) Connect and tighten the cables allowing tension at the load spreader attached to the actuator,
9) Retract the actuator to the starting position,
10) Retract the actuator to 0.050 in. above the starting position,
11) Return to the starting position,
12) Repeat the loading cycle, incrementing the displacements until something big (cracking or metal binding) occurred,
13) Upward loading was not allowed to exceed an applied tension greater than around 3000 pounds for fear of breaking the lifting cables,
14) After testing, the actuator was moved to a position which applied no load and the load spreader and actuator connections were disassembled,
15) The piston was retracted fully,
16) The instrumentation was removed,
17) The end cables were removed, and
18) The pipe was taken off the test stand and returned to its cradle.

The loading on the compression side was applied through rollers; the loading on the tension side was applied by wire rope cables in line with the rollers. The test was performed in displacement control. Measuring devices included two +/- 0.5 in. DCDTs, one mounted on top of the pipe spanning the gap and one mounted below the pipe spanning the gap for tests with a gap. For tests with a jointed pipe the DCDTs were mounted such that displacements were measured at the bell of a pipe section. A clinometer was mounted near the DCDTs at the pipe spring line. The piston was extended to just short of touching the loading system, then the data gathering system was started. Data was gathered at 10 Hz with an NI-SCXI/PXI combination using an NI-1520 signal conditioning card to condition the DCDTs and clinometer. The force and actuator displacement signals are conditioned in the Flextest SE servo-controller. The sensitivity of the displacement manual commands was set at 0.001 in. and the actuator was incremented to 0.05 in. displacement, then returned to start, then retracted to 0.05 in., and finally returned to starting position. The

second cycle was performed with target displacements of +/- 0.1 in. (0.002 in. step size), then 0.15 in. (0.005 in. step size from here on), until the target displacements were reached.

The rotation angles were calculated from the DCDTs using:

$$\theta\,(degrees) = tan^{-1}\left[\frac{(\,top\ disp.-bottom\ disp.)}{distance\ between\ centers\ of\ DCDTs=8.9in.}\,\frac{180^0}{\pi}\right] \tag{8}$$

The angle was also calculated from the piston displacement using:

$$\theta\,(degrees) = tan^{-1}\left[\frac{1*(\,actuator\ displacement)}{(distance\ between\ top\ loading\ points=28in.)/2}\,\frac{180^0}{\pi}\right] \tag{9}$$

4. Data and Results

Table 1 lists the general characteristics of each four-point bending test. The maximum tension force was limited to 3 kips, which was the maximum force allowed on the stranded cables used to pull the pipe upward.

Table 1. Bending Test Specimens

Specimen	Date Tested	Liner	Load Centered On	Maximum Displacement (in.)[a]	Maximum Force (kips)[b]
1	March 04, 2011	Unbonded	Joint	- 0.68[c] + 0.3	+ 6.2 - 3.0
2	March 04, 2011	Unbonded	Joint	- 0.79 + 0.3	+ 10.5 - 3.0
3	Feb. 02, 2011 March 02, 2011	Unbonded	Gap	± 0.30	± 1.5
10	March 04, 2011	Bonded	Joint	- 0.39[c] - 1.07 + 0.1	+ 6.5 + 11.8 -3.0
12	March 03, 2011	Bonded	Gap	- 0.5 + 0.25	+ 3.6 -3.0

a – Downward Displacement is Negative b – Compressive Force is Positive

c – Liner First Cracks

The pipes were initially displaced downward in increments, then moved upward to a small displacement without exceeding the maximum cable load, and finally moved to a zero displacement condition. The aforementioned steps were repeated for each test set. It is important to note that for

all test cycles there was a residual tension (upward) force in the actuator when the pipe was returned to the zero displacement condition, which is recorded in the Target Test Regimen Table (see Tables 2 through 6) for each individual specimen.

The force recorded during these tests and displayed for each force-displacement figure in this report is the incremental downward force required to achieve the prescribed displacement and is different than the maximum compressive force. The incremental force shown in these figures is based on starting the downward movement at the residual tension force necessary to return the pipe to the zero displacement position.

4.1 Specimen 1

Specimen 1 had an unbonded liner with the joint at the center of the test specimen. The planned test regime and force-displacement results for Specimen 1 are given in Table 2 and Figure 3, respectively.

Table 2. Target Test Regimen for Specimen 1

Test Cycle	Down (in.)	Up (in.)	Residual Force @ End of Cycle (kips)
1	0.05	0.05	0
2	0.10	0.10	0.08
3	0.15	0.15	0.12
4	0.20	0.20	0.16
5	0.25	0.25	0.19
6	0.30	0.30	0.17
7	0.40	0.40	0.17
8	0.50	N/A	-0.23
8	0.60	N/A	N/A
8	0.70	0.10	N/A

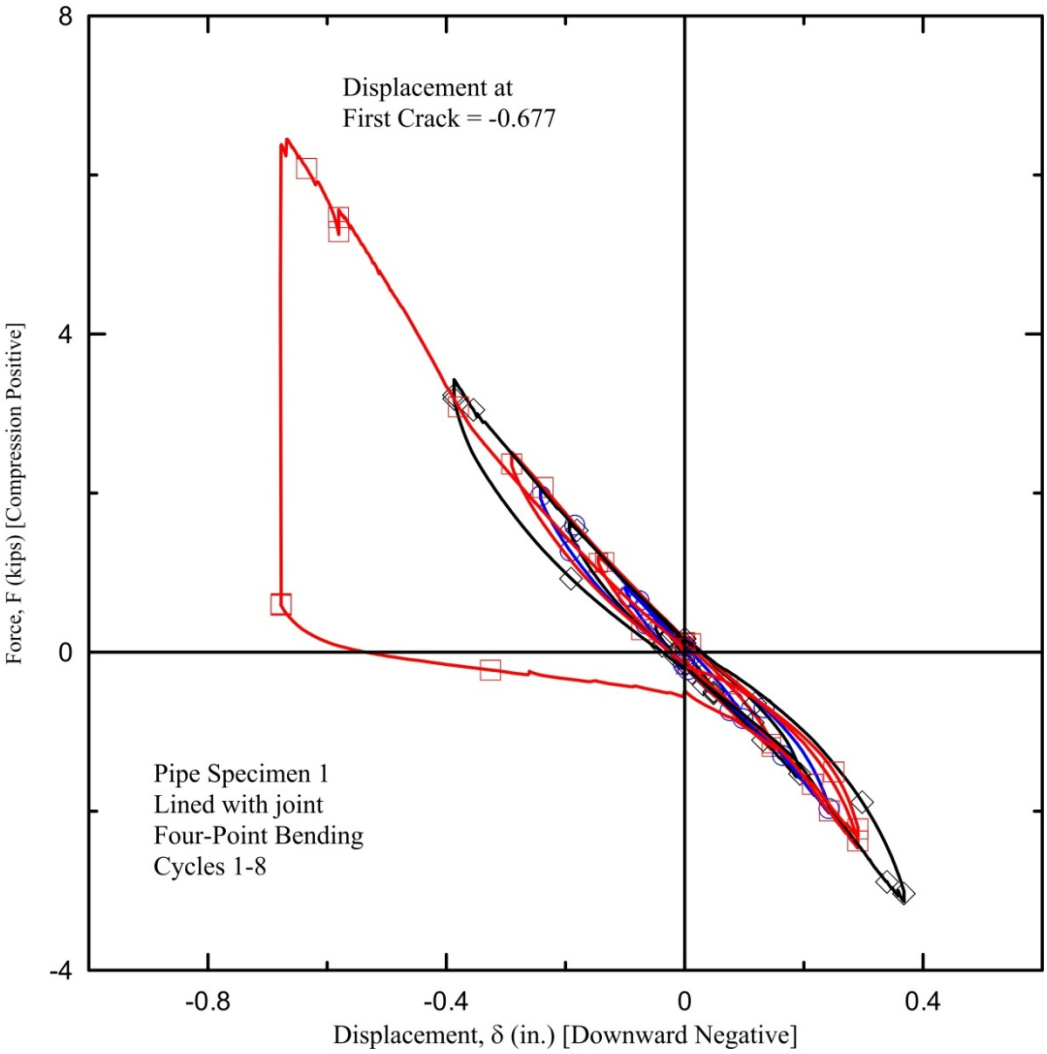

Figure 3. Force vs. Displacement for Specimen 1

At a downward displacement of -17.3 mm (-0.68 in.) there was an audible pop and immediate reduction of applied force. This force reduction is clearly shown in Figure 3, and represents the initial cracking of the liner in tension at the bottom of the test specimen. Photo 2 illustrates the crack in the liner. The compressive force exerted by the actuator at the time of the liner break (see Table 1) was F = 27.6 kN (6.2 kips). This agrees favorably with the calculated breaking force of 27.7 kN (6.23 kips) found using the geometries and flexural strength given in Section 2.

Photo 2. Image of Specimen 1 Liner after First Rotation Testing
Showing a Crack at the Center

Figure 4 shows the peak points from the individual cycles 1 through 7, along with the complete force–displacement results for cycle 8. Cycles 1 through 7 peak data follow the trend line for cycle 8.

Similarly, Figure 5 shows the moment–rotation results based on the peak points from the individual cycles 1 through 7, along with the complete moment-rotation results of cycle 8 for Specimen 1. Data in Figure 5 follow the same trends as in Figure 4 since both moment and rotation are linear functions of force and displacement, respectively. Rotation data in Figure 5 are based on measurements from the DCDTs, as described in section 3 of this report.

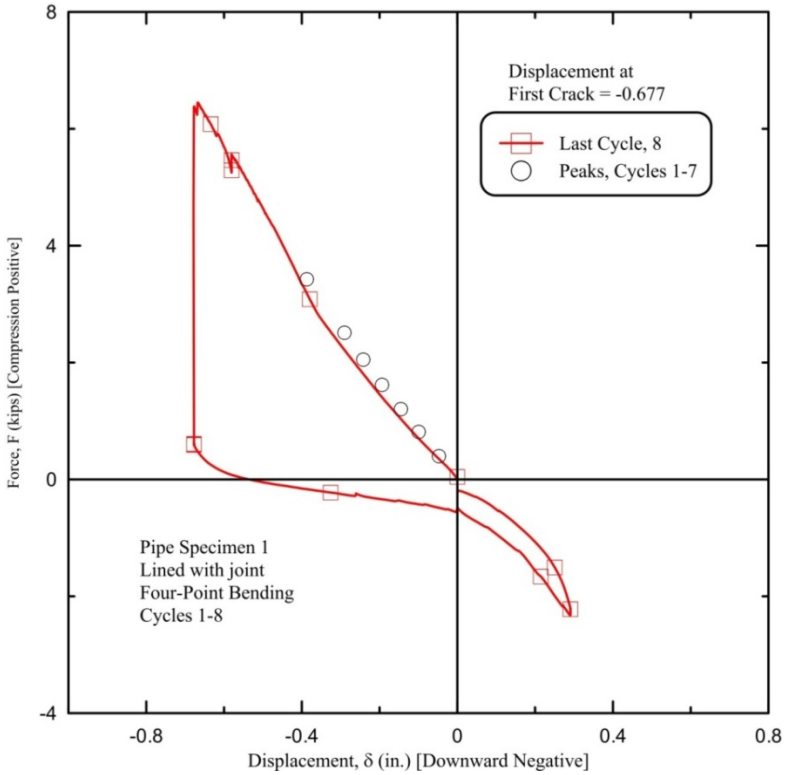

Figure 4. Peak Force vs. Displacement for Specimen 1

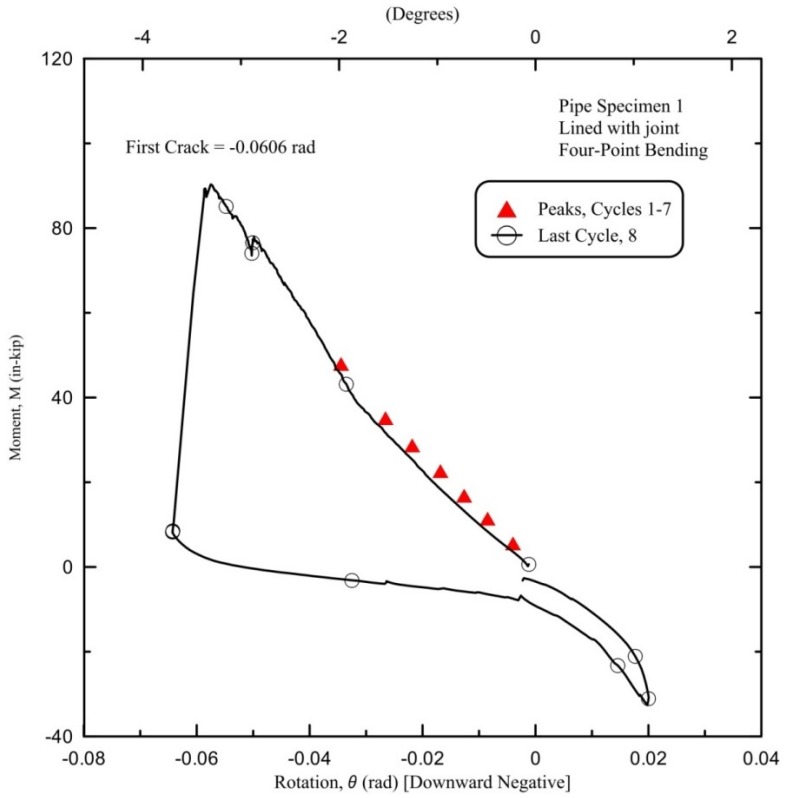

Figure 5. Moment vs. Rotation for Specimen 1

4.2 Specimen 2

Similar to Specimen 1, Specimen 2 had an unbonded liner with its joint centered in the test apparatus. The planned test regime and residual tension force of each test cycle for Specimen 2 are given in Table 3.

Figure 6 shows the force-displacement results of Specimen 2. At a downward displacement of -19.4 mm (-0.765 in.) there was an audible pop and an immediate reduction of applied force. This force reduction is clearly shown in Figure 6 and represents an initial cracking of the liner in tension at the bottom of the test specimen. Photo 3 shows the crack in the liner. The compressive force exerted by the actuator at the time of the liner break (see Table 1) was F = 46.7 kN (10.5 kips), which is significantly greater than the calculated breaking force of 27.7 kN (6.23 kips).

Table 3. Target Test Regimen for Specimen 2

Test Cycle	Down (in.)	Up (in.)	Residual Force @ End of Cycle (kips)
1	0.05	0.05	-0.23
2	0.10	0.10	-0.21
3	0.15	0.15	-0.16
4	0.20	0.20	-0.16
5	0.25	0.25	-0.13
6	0.30	0.30	-0.12
7	0.40	0.25	-0.22
8	0.50	N/A	-0.51
8	0.60	N/A	N/A
8	0.70	N/A	N/A
8	0.75	N/A	N/A
8	0.77	0.30	N/A

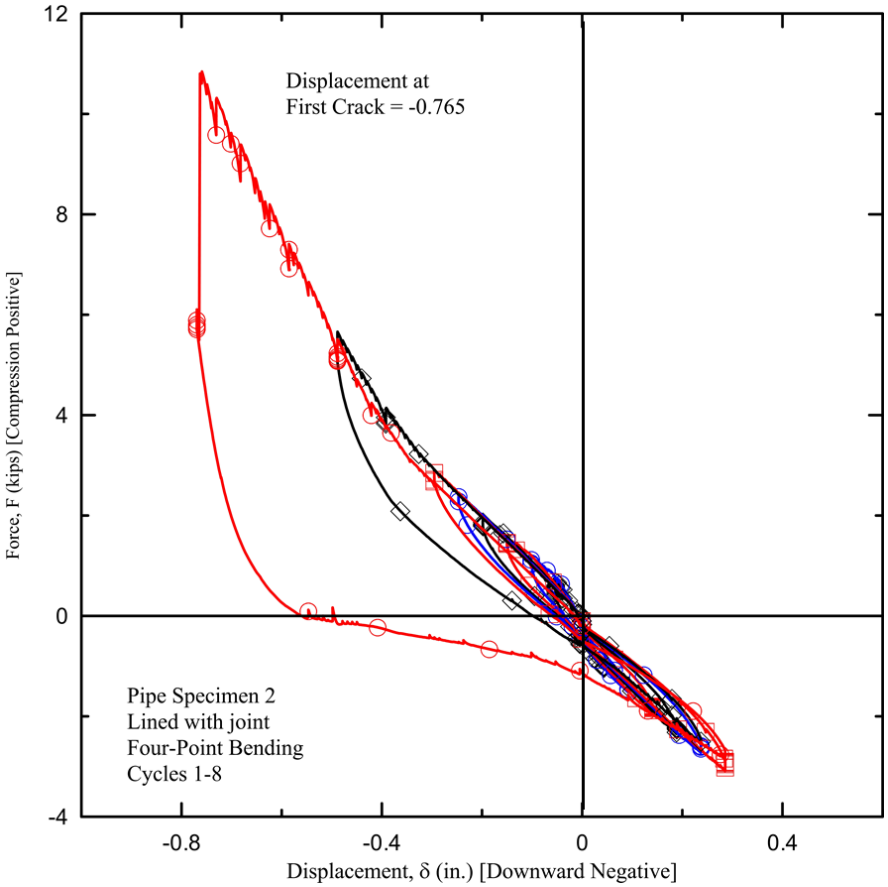

Figure 6. Force vs. Displacement for Specimen 2

Photo 3. Image of the Specimen 2 Liner after First Rotation Testing Showing a Crack at the Center

Figure 7 shows the peak points from the individual cycles 1 through 7, along with the complete force–displacement results for cycle 8. Cycles 1 through 7 peak data follow the trend line for cycle 8. Figure 8 illustrates moment–rotation results based on the peak points in the load cycles for Specimen 2. Rotations in Figure 8 are based on the data from DCDTs.

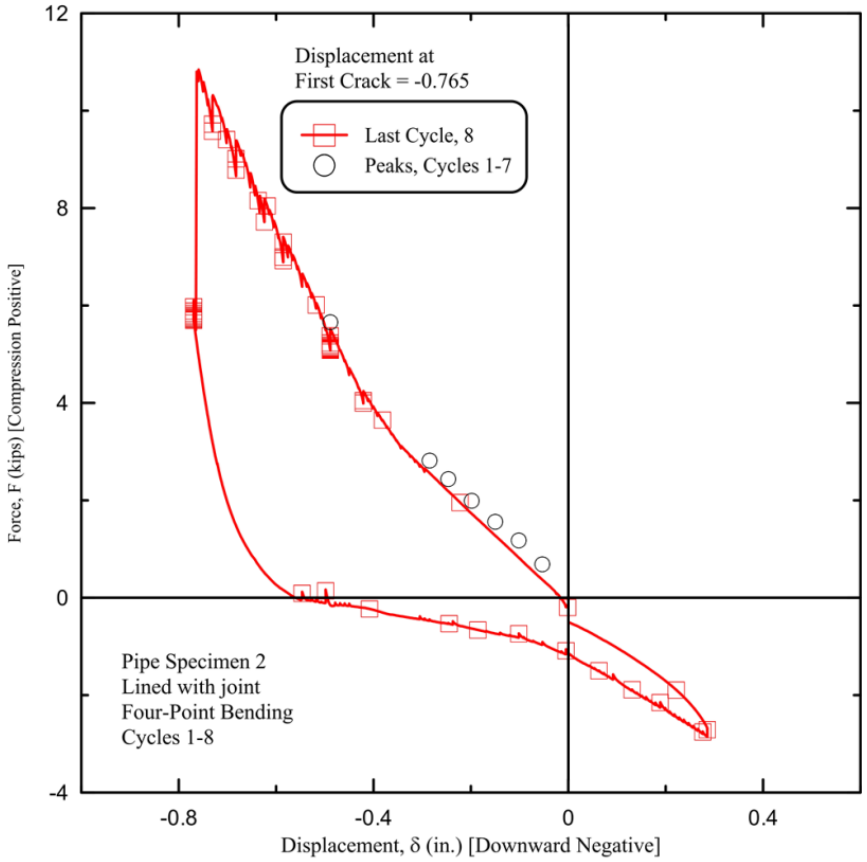

Figure 7. Peak Force vs. Displacement for Specimen 2

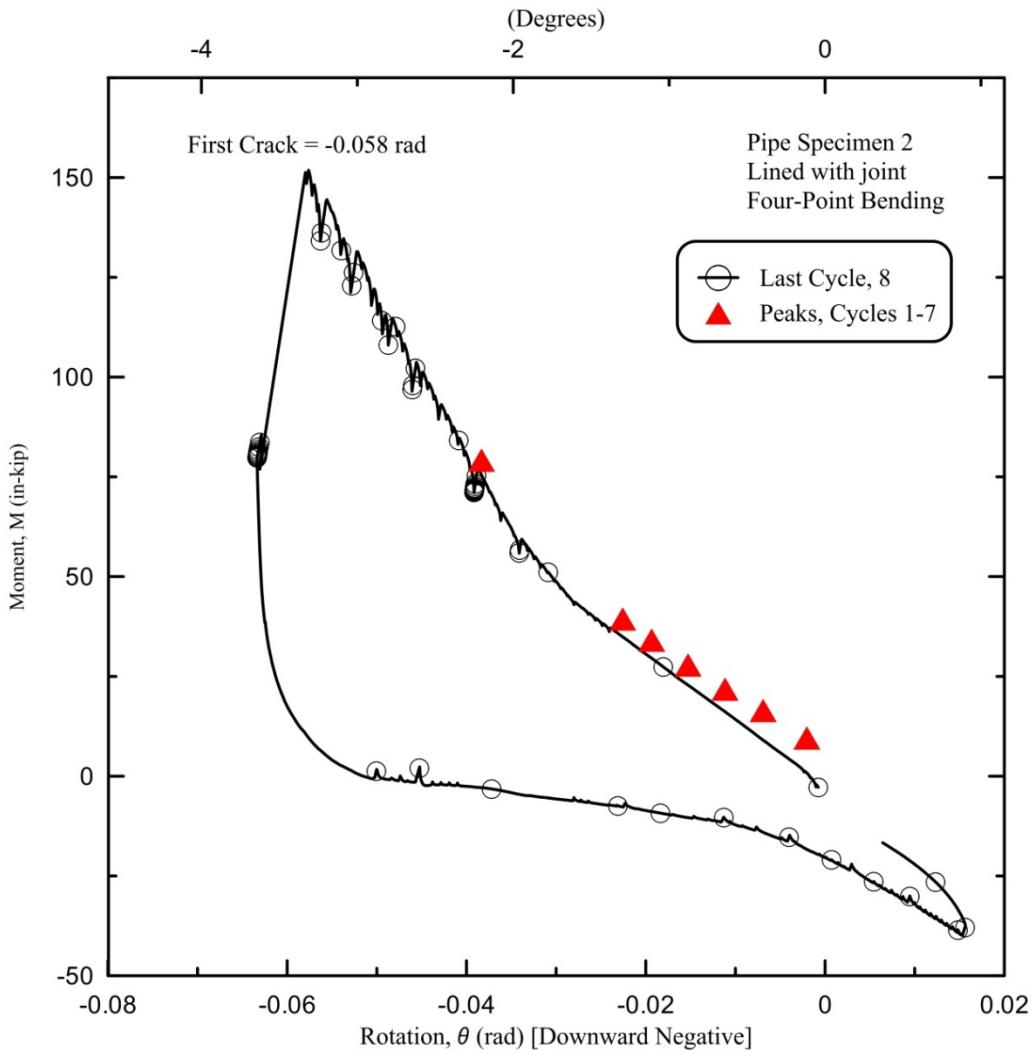

Figure 8. Moment vs. Rotation for Specimen 2

4 .3 Specimen 3

Specimen 3 had an unbonded liner with a circumferential gap at the center of the test specimen. The planned test regime for Specimen 3 is given in Table 4.

Figure 9 and Figure 10 show the force-displacement results of Specimen 3 for cycles 1 through 5 and 6 through 10, respectively. The force in Figure 9 and Figure 10 is the incremental downward force required to achieve the displacement.

Table 4. Target Test Regimen for Specimen 3

Test Cycle	Down (in.)	Up (in.)	Residual Force @ End of Cycle (kips)
1	0.05	0.05	-0.024
2	0.1	0.1	-0.011
3	0.15	0.15	0.020
4	0.2	0.2	0.074
5	0.25	0.25	-0.004
6	0.05	0.05	-0.075
7	0.1	0.1	-0.035
8	0.15	0.15	-0.029
9	0.25	0.25	-0.046
10	0.3	0.3	-0.031

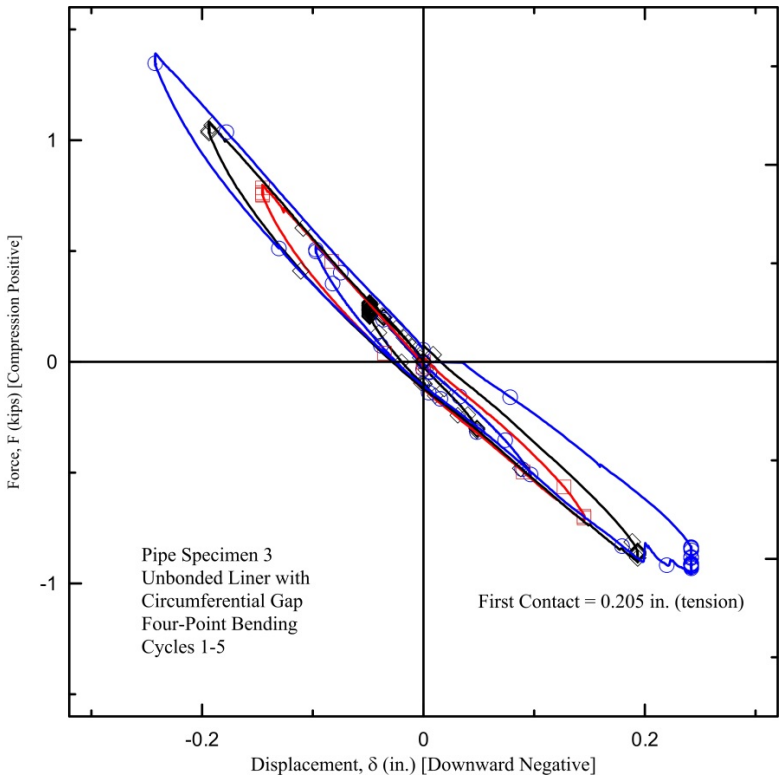

Figure 9. Force vs. Displacement for Cycles 1-5, Specimen 3

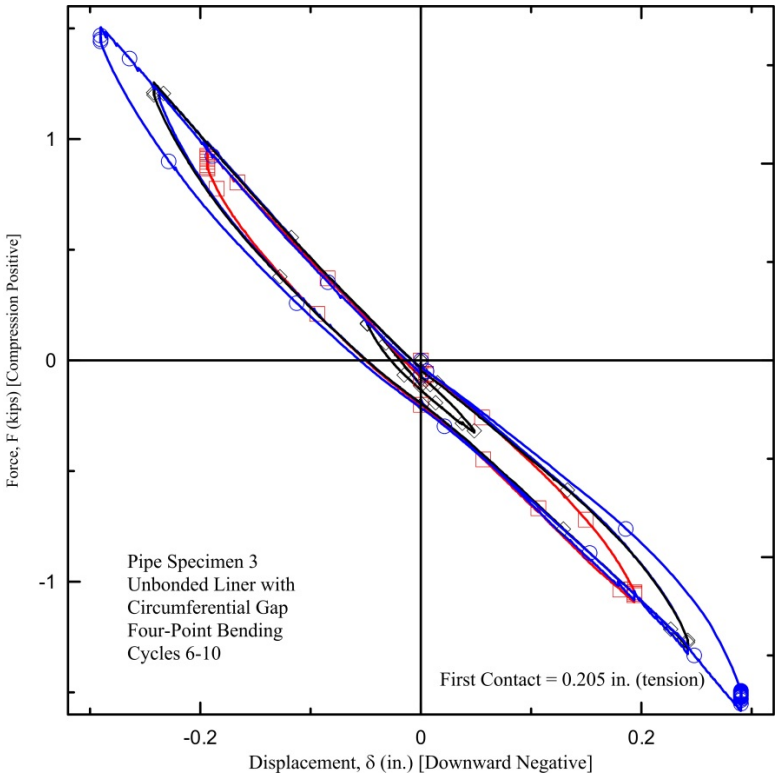

Figure 10. Force vs. Displacement for Cycles 6 – 10, Specimen 3

At an upward displacement of 5.21 mm (0.205 in.) the first contact took place across the gap at the bottom of the pipe. This metal to metal contact between the two segments of pipe is referred to as gap closure. Discerning the behavior of the liner beyond this point becomes more complicated because the center of rotation shifts to the location of binding. The tensile force applied at metal binding was -3.78 kN (-0.85 kips). Photo 4 shows the inner part of the liner confirming the absence of a crack. The maximum compressive force exerted by the actuator at the time contact was noticed was F = 6.67 kN (1.5 kips) (see Table 1).

Photo 4. Image of Specimen 3 Liner after First Rotation Testing Showing No Crack

Figure 11 shows the peak points from the individual cycles 1 through 9, along with the complete force-displacement results for cycle 10. It is noted that before the first contact, which took place during cycle 5, the peak force required for each targeted downward displacement is slightly greater than the peak force required for the same targeted displacement after cycle 5. The peak points of cycles 6 through 9 are consistent with the complete force–displacement results from cycle 10.

Figure 12 shows the moment–rotation results based on the peak points in the load cycles for Specimen 3. The rotations in Figure 12 are based on data from the DCDTs.

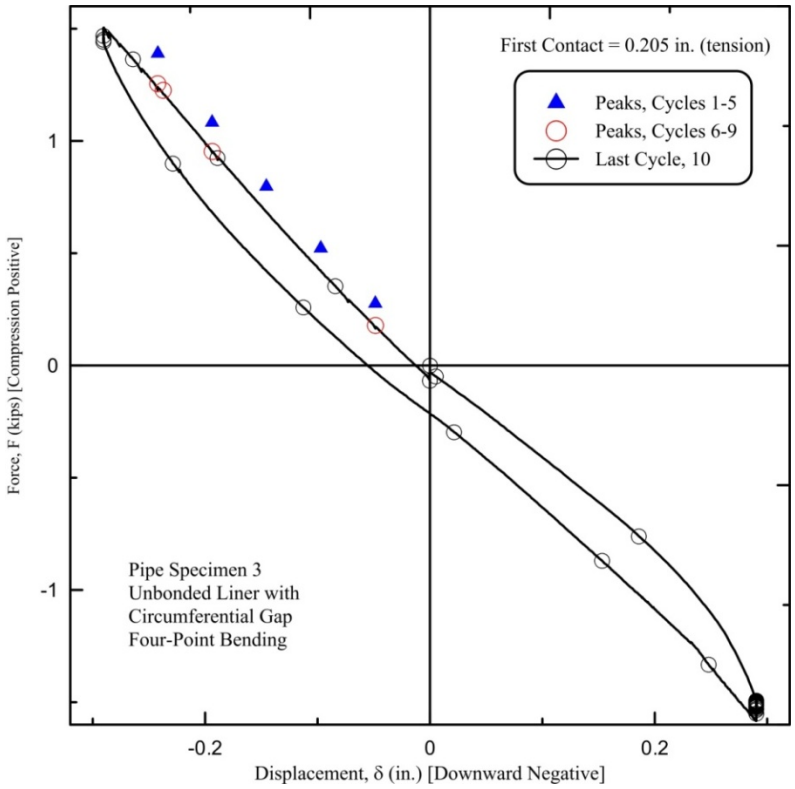

Figure 11. Peak Force vs. Displacement for Specimen 3

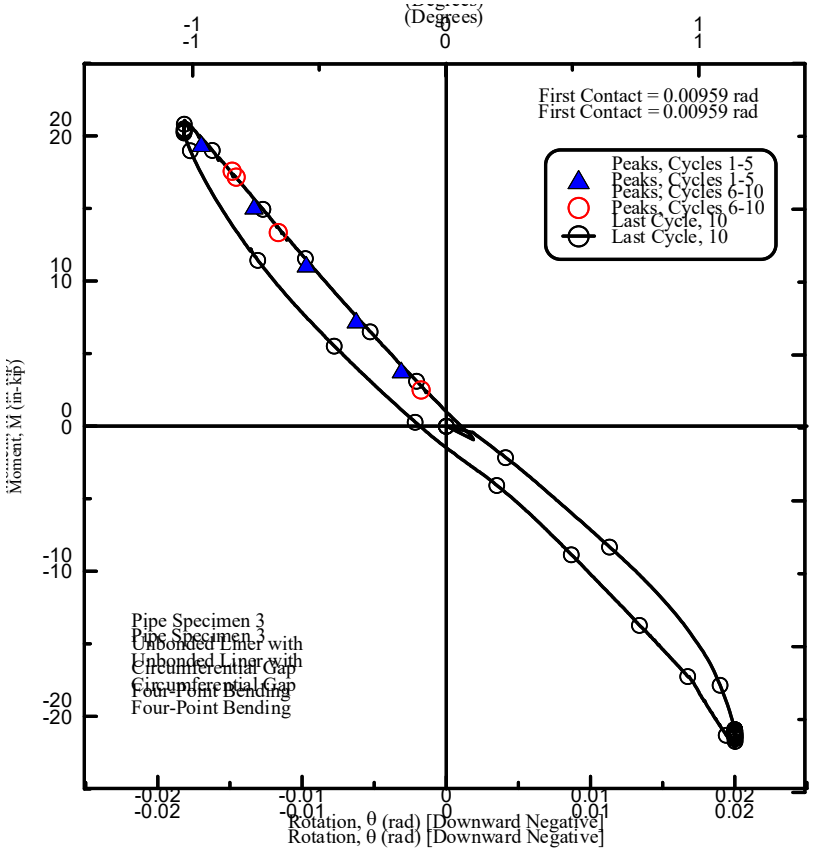

Figure 12. Moment vs. Rotation for Specimen 3

4.4 Specimen 10

Specimen 10 had a bonded liner with the joint at the center of the test specimen. The planned test regime for Specimen 10 is given in Table 5. Figure 13 shows the force-displacement results for the first seven cycles of Specimen 10.

Table 5. Target Test Regimen for Specimen 10

Test Cycle	Down (in.)	Up (in.)	Tension @ End of Cycle (kips)
1	0.05	0.05	0
2	0.10	0.10	-0.07
3	0.15	0.10	-0.28
4	0.20	0.10	-0.28
5	0.25	0.10	-0.37
6	0.30	0.10	-0.40
7	0.40	0.10	-0.45
8	0.50	0.10	-0.65
9	0.60	0.10	-0.61
10	0.70	0.10	-0.60
11	0.80	NA	-0.63
11	0.90	NA	NA
11	1.00	NA	NA
11	1.10	0.10	NA

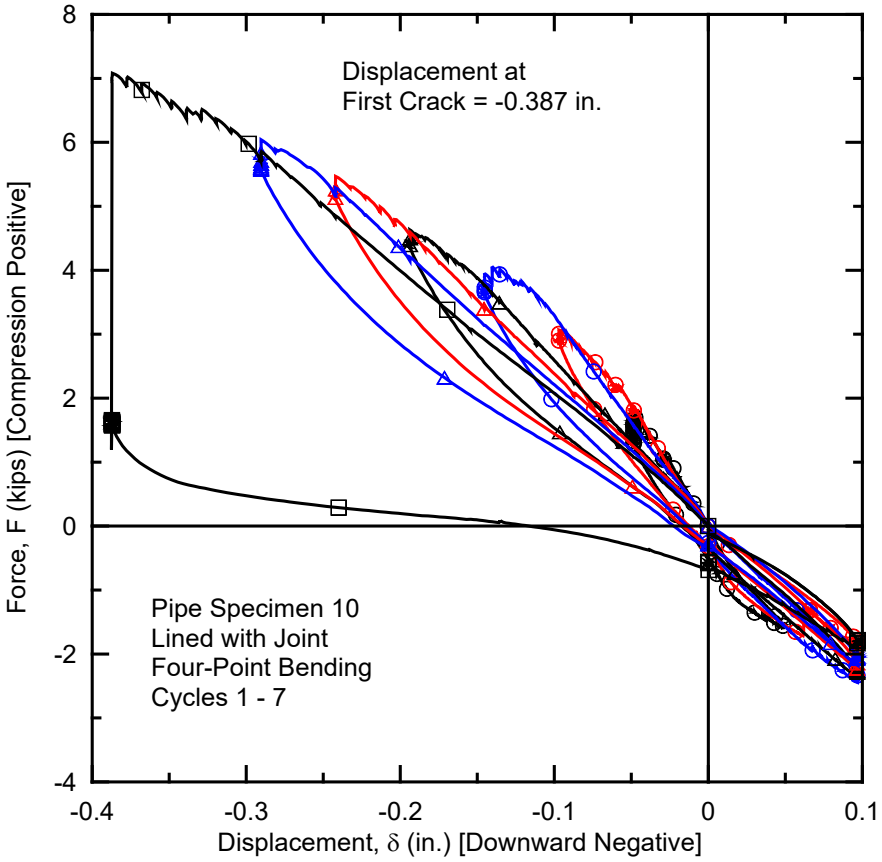

Figure 13. Force vs. Displacement for Cycles 1 – 7, Specimen 10

At a downward displacement of -9.91 mm (-0.39 in.) there was an audible pop with an immediate reduction of the applied force. This force reduction is clearly shown in Figure 13, and represents an initial cracking of the liner in tension at the bottom of the test specimen. Photo 5 shows the crack in the liner. The compressive force exerted by the actuator at the time of the liner break (see Table 1) was F = 28.9 kN (6.5 kips). This agrees favorably with the calculated breaking force presented in Section 2.

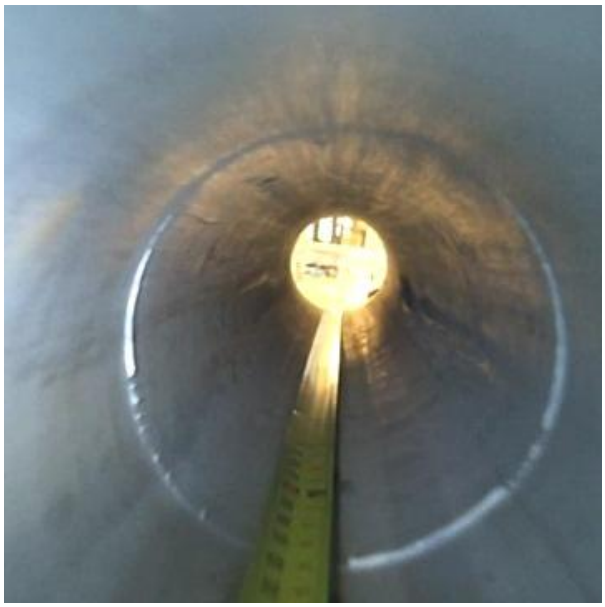

Photo 5. Image of Specimen 10 Liner after First Rotation Testing
Showing a Crack at the Center

Figure 14 shows the incremental force–displacement data for cycles 8 through 11 for test Specimen 10. The curves have distinctively steeper slopes after the first crack at a displacements of -9.91 mm (-0.39 in.).

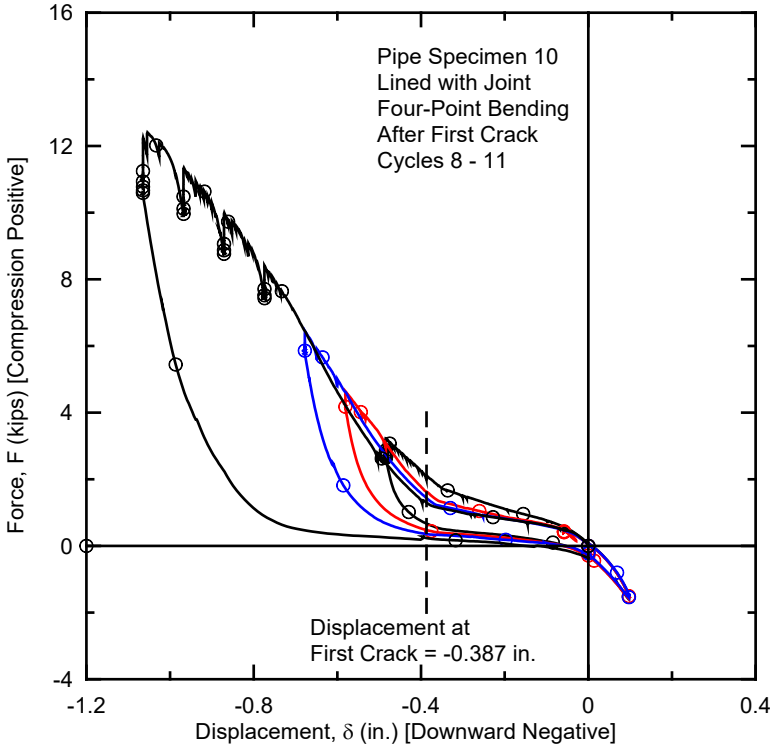

Figure 14. Force vs. Displacement for Cycles 8 - 11, Specimen 10

Figure 15 shows the peak points from the individual cycles 1 through 10, along with the complete force–displacement results for cycle 11. Cycles 1 through 7 peak data show a clear trend of a "backbone" force–displacement curve. Following the first cracking at δ = -9.91 mm (-0.39 in.), the peak points of cycles 8 through 10 are consistent with the complete force–displacement results from cycle 11.

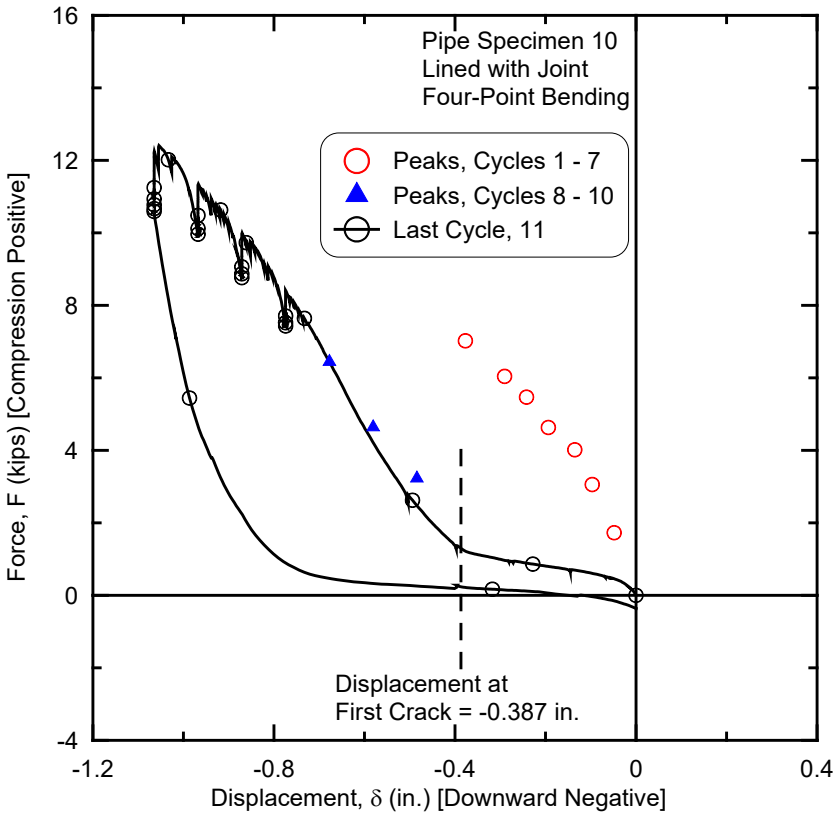

Figure 15. Peak Force vs. Displacement for Specimen 10

Figure 16 shows the moment–rotation results based on the peak points in the load cycles for Specimen 10. These data follow the same trends as in Figure 15 since both moment and rotation are linear functions of force and displacement, respectively. The rotations in Figure 16 are based on clinometer data.

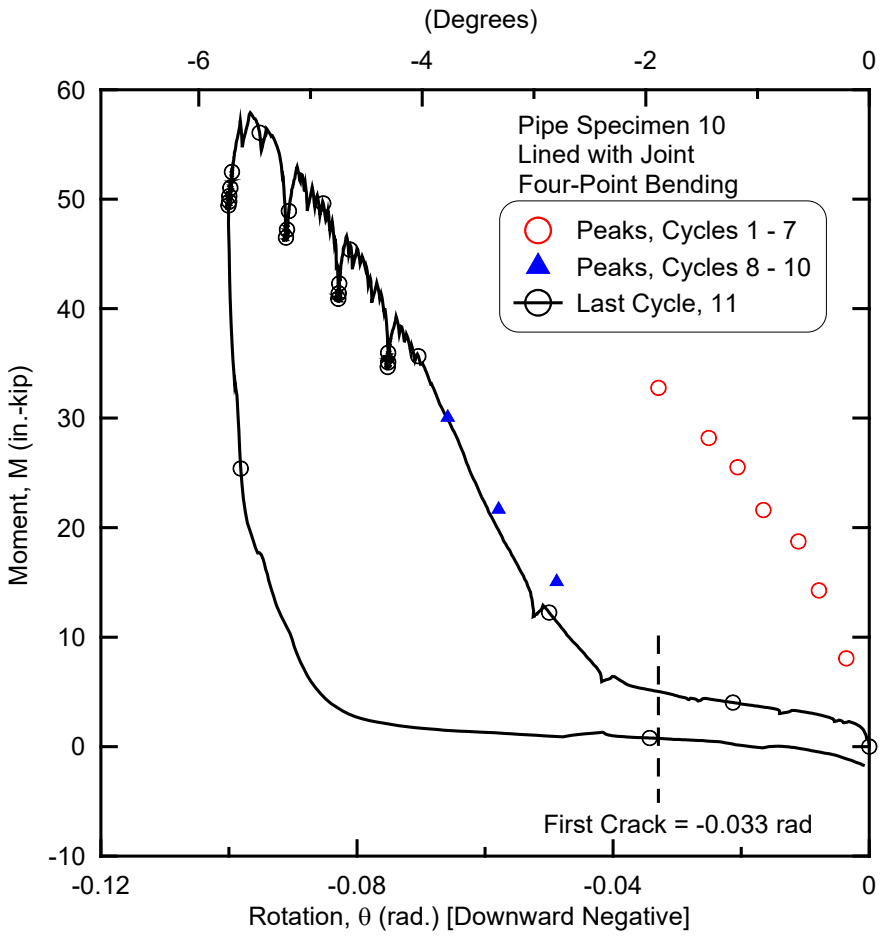

Figure 16. Moment vs. Rotation for Specimen 10

4.5 Specimen 12

Specimen 12 had a bonded liner with a full circumferential gap at the center of the test specimen. The planned test regime and force-displacement results for Specimen 12 are presented in Table 6 and Figure 17, respectively.

At a downward displacement of -11.94 mm (-0.47 in.) an abrupt reduction of the applied force is observed (Figure 17). The compressive force exerted by the actuator at the time of contact (see Table 1) was F = 16.0 kN (3.6 kips). Photo 6 verifies that this reduction in force does not represent complete cracking of the liner because no visual indication of failure is observed inside the pipe. It is not certain whether an unseen portion of the liner failed or that the bond between DI and mortar or mortar and IMain liner ruptured causing slip along their respective interface. Also note, when Specimen 12 was lined by InsituForm it was the last specimen at the end of the bonded sections.

Table 6. Target Test Regimen for Specimen 12.

Test Cycle	Down (in.)	Up (in.)	Residual Force @ End of Cycle (kips)
1	0.05	0.05	-0.0293
2	0.1	0.1	-0.0002
3	0.15	0.15	0.0514
4	0.2	0.2	-0.0035
5	0.25	0.2	-0.0004
6	0.35	0.3	-0.0007
7	0.4	0.3	-0.0293
8	0.45	0.3	-0.0749
9	0.5	0	-0.0749

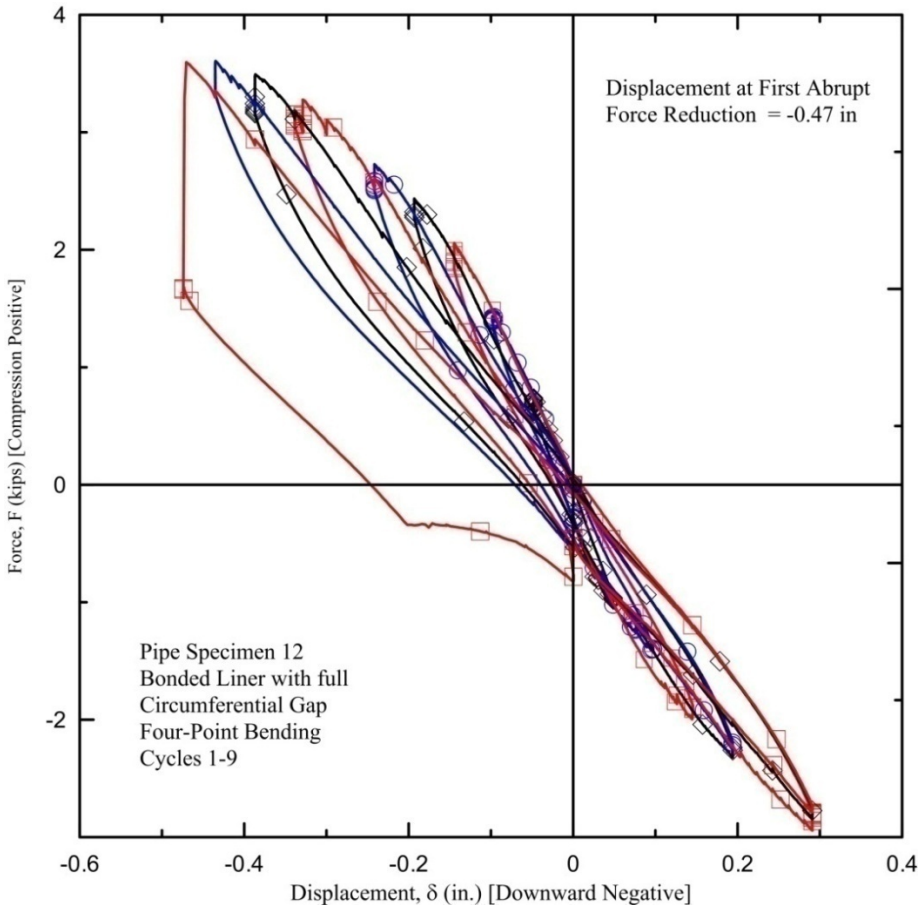

Figure 17. Force vs. Displacement for Specimen 12

Photo 6. Image of the Specimen 12 Liner after First Rotation Testing

Figure 18 shows the peak points from the individual cycles 1 through 8, along with the complete force–displacement results for cycle 9. Cycles 1 through 8 peak data show a clear trend of a "backbone" force–displacement curve. Figure 19 shows the moment–rotation results based on the peak points in the load cycles for Specimen 12. The rotations in Figure 19 are based on data from the DCDTs.

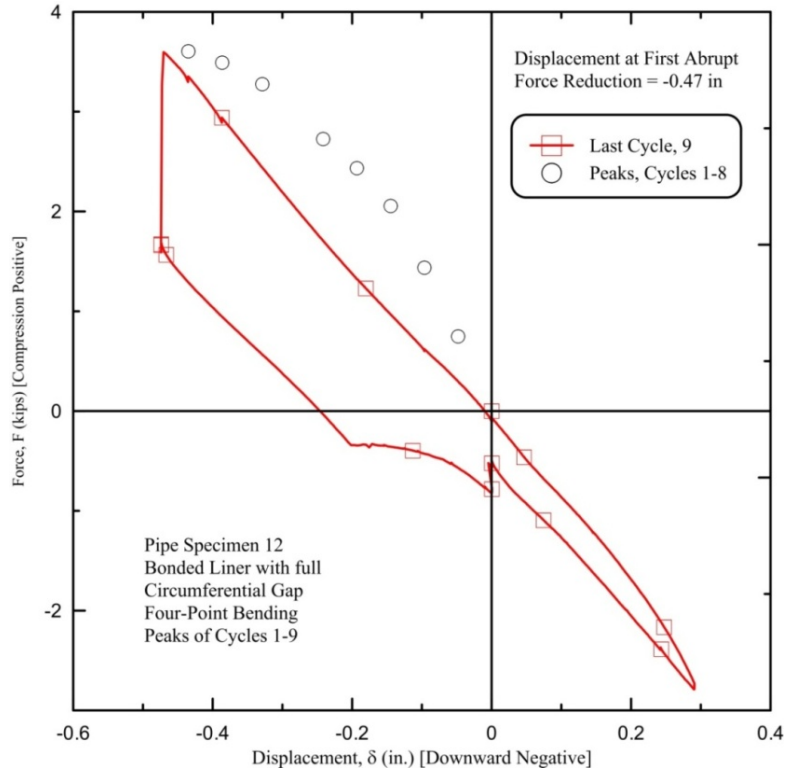

Figure 18. Peak Force vs. Displacement for Specimen 12

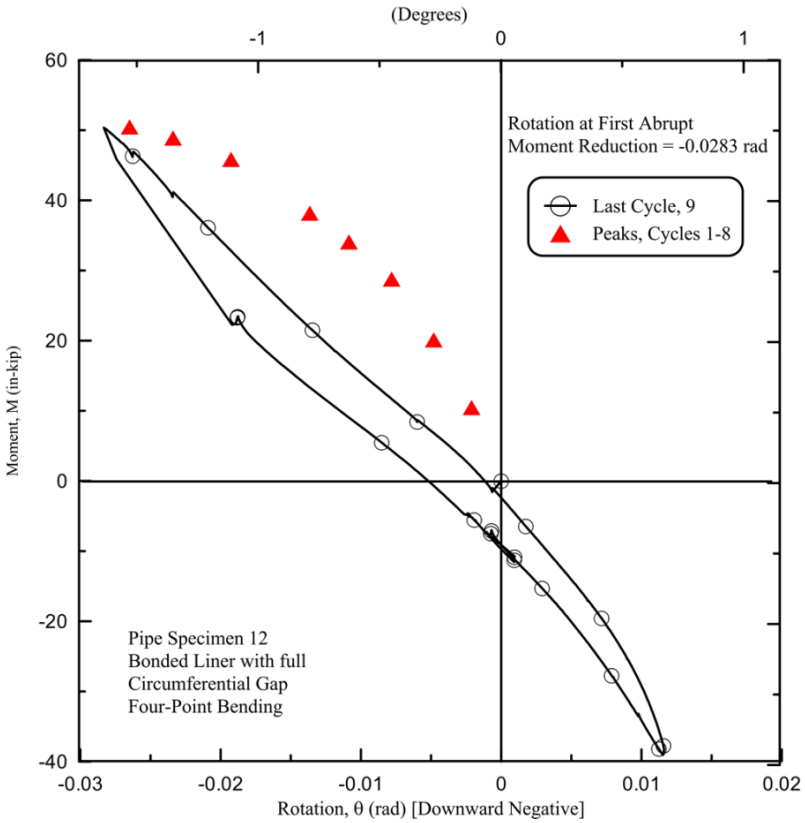

Figure 19. Moment vs. Rotation for Specimen 12

5. Discussion of Results

Specimen 1 had an unbonded liner. The four-point bending test resulted in a crack in the liner at a downward displacement of approximately -17.3 mm (-0.68 in.). The outer fiber tensile bending stress estimated at the point the crack occurred agreed favorably with the data supplied by InsituForm for the IMain liner.

Specimen 2 had an unbonded liner. The four-point bending test resulted in a crack in the liner at a downward displacement of approximately -19.4 mm (-0.765 in.). The outer fiber tensile bending stress estimated at the point of cracking was about 1.7 times greater than the force derived from the data supplied by InsituForm for the IMain liner.

Figure 20 illustrates force-displacement based on peak points in the load cycles for Specimens 1 and 2. To calculate the initial bending stiffness, EI, of the two specimens, Equation 2 is utilized. Applied force and the resulting displacement of the first cycle were used to calculate this parameter. As shown in Table 7, Specimen 1 has an initial bending stiffness EI = 88,800 kips-in^2, whereas Specimen 2 has EI = 136,000 kips-in^2. Despite being identical specimen types and cracking at comparable downward displacements, the applied force at cracking for these specimens varies significantly. This difference in the failure force may be attributed to several factors including inconsistencies in the quality of unbonding between the liner and mortar. If some liner to mortar bonding was generated in Specimen 2 it would account for the difference in bending stiffness and flexural strength between the specimens.

Table 7. Summary of Approximate Specimen Stiffness

Specimen	Liner	Load Centered On	EI (kips-in^2)
1	Unbonded	Joint	88,800
2	Unbonded	Joint	136,000
3	Unbonded	Gap	60,000
10	Bonded	Joint	376,000
12	Bonded	Gap	164,000

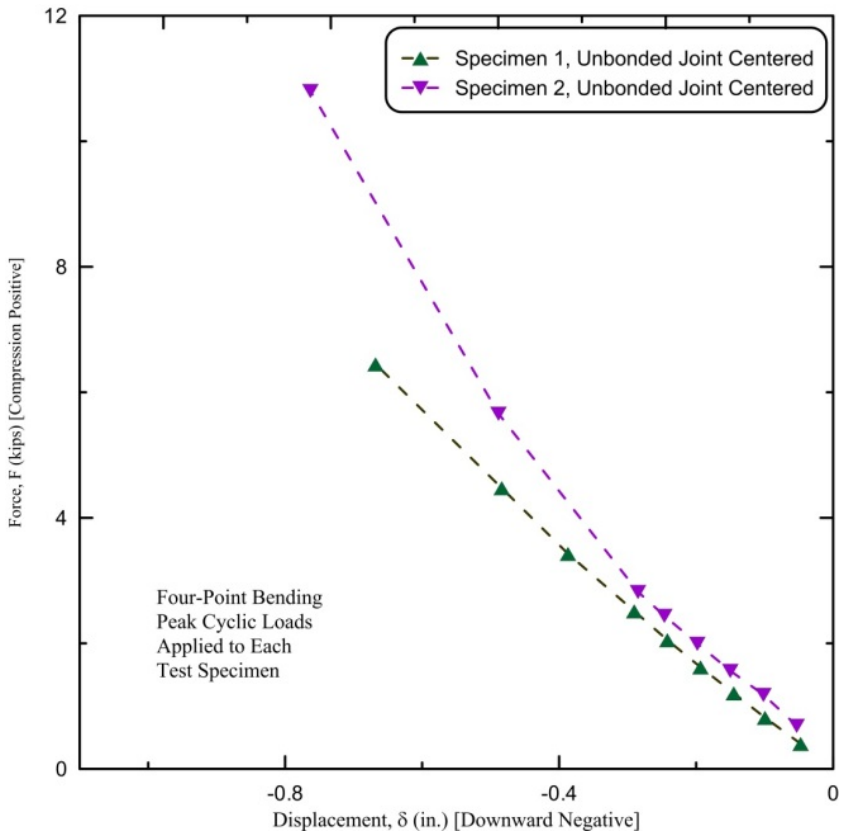

Figure 20. Force-displacement based on peak points for Specimens 1 and 2.

Specimen 10 had a joint centered fully bonded liner. The four-point bending test resulted in a crack in the liner at a downward displacement of approximately -9.91 mm (-0.39 in.). The outer fiber tensile bending stress estimated at the point of cracking agreed favorably with the data supplied by InsituForm for the IMain liner. Following the initial cracking of the liner, substantial additional bending capacity was developed. The force-displacement curve beyond the first crack did not follow the trend established prior to cracking. This observation can be attributed to the resisting force developed by bell and spigot contact. Specimen 10 had an initial bending stiffness EI = 376,000 kips-in^2.

Figure 21 illustrates force-displacement results based on peak points of load cycles for Specimens 1, 2 and 10. Specimen 10, which is bonded, has a greater initial bending stiffness than the unbonded specimens. The liner cracks at approximately half the displacement of liners in Specimens 1 and 2. The applied force when the liner cracks is 28.9 kN (6.5 kips), which corresponds well with the force required to crack the liner of Specimen 1 and the value provided by InsituForm.

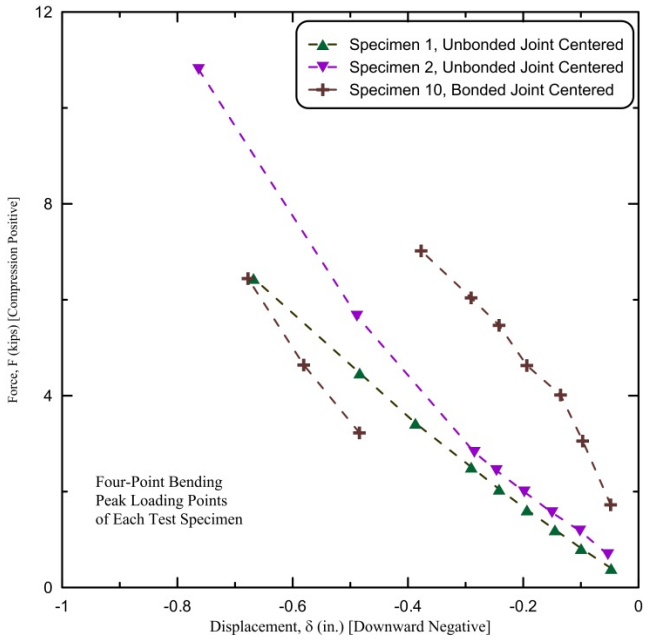

Figure 21. Force-displacement based on peak points for Specimens 1, 2 and 10

Specimen 3 had an unbonded liner with a circumferential gap at the center of the test specimen. At an upward displacement of 5.21 mm (0.205 in.) the first contact took place at the bottom of the pipe.

The force applied at this point of the test was -3.78 kN (-0.85 kips) while the maximum compressive force exerted by the actuator was F = 6.67 kN (1.5 kips). Specimen 3 produced an initial bending stiffness EI = 60,000 kips-in^2.

Specimen 12 had a bonded liner with the full circumferential gap at the center of the test specimen. At a downward displacement of -11.94 mm (-0.47 in.) an abrupt reduction of the applied force was observed. This force reduction does not represent cracking of the liner, as discussed in section 4.5. The compressive force exerted by the actuator at the time of the applied force reduction was F = 16.0 kN (3.6 kips). Specimen 12 has initial bending stiffness EI = 164,000 kips-in^2. The force-displacement results based on peak points in load cycles for Specimens 3 and 12 are presented in Figure 22. The additional stiffness and strength provided by the mortar-liner bond is clearly illustrated by the figure.

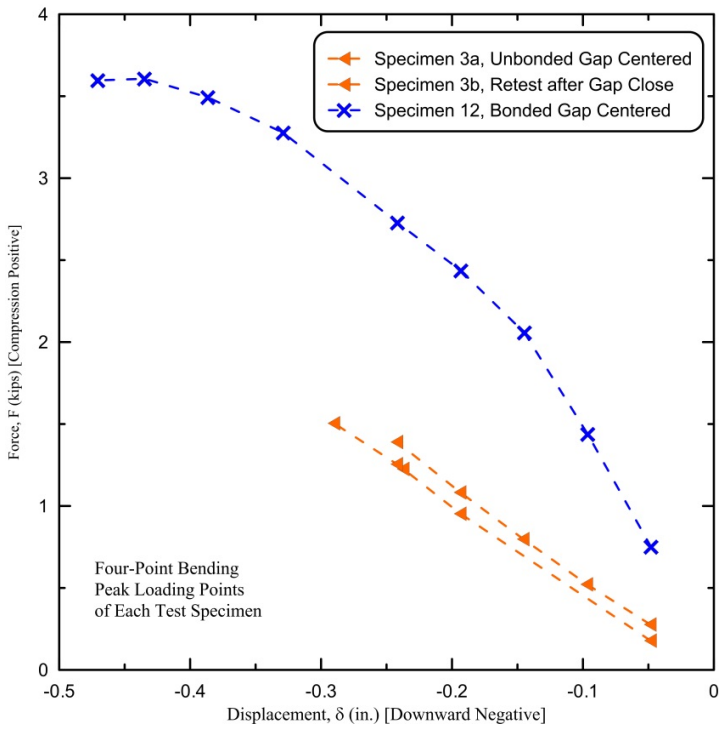

Figure 22. Force-displacement based on peak points for Specimens 3 and 12

6. Summary and Recommendations

Liner failure in the specimens that had full circumferential gaps at their center could not be fully characterized because they experienced gap closure before failure of the liner. However, these tests did provide data regarding the initial behavior of the liner at the location of a pipe fracture under applied bending.

Unbonded and joint centered specimens exhibit more ductile behavior in bending than other tested configurations as demonstrated by their ability to resist larger imposed displacements. At this time we have not drawn definitive conclusions regarding the bending stiffness of these specimens because this parameter depends on several factors including the extent and characteristics of bonding between the liner and mortar.

To achieve an accurate estimate of the bending stiffness of the composite cross-section for both bonded and unbonded specimens additional tests are recommended. Supplementary jointed specimens need to be subjected to bending tests to determine more accurately the displacement at which the liner cracks and its corresponding bending stiffness. More precise estimates of the bending stiffness and stress-strain curves of the composite section may be necessary for future finite element analysis.